Integrating trophic interactions into projecting distribution changes in marine fishes

Jose A. Fernandes, William W.L. Cheung, Simon Jennings, Momme Butenschön, Lee de Mora, Thomas L. Frölicher, Manuel Barange, Alastair Grant

Abstract

Climate change is affecting the distribution and abundance of marine fishes and invertebrates. Bioclimate envelope approaches have been used to predict changes in the distribution of multiple species on large spatial scales but presently do not account for the effects of intra- and inter-specific competition for resources among species. In this paper, we develop and test a modelling approach that combines a species-based dynamic bioclimate envelope model with a size-based model to predict the effects of competition for resources on redistribution. Model predictions for 1970 to 2004 were computed using outputs from two different model systems applied to the North Atlantic basin: the NOAA's Geophysical Fluid Dynamic Laboratory ESM2.1 model (GFDL) and the European Regional Seas Ecosystem Model (ERSEM). The results were challenged with data describing variability in the abundance of 24 of the most abundant fishes in the North Atlantic. The results show that considering species interactions in the model increases the goodness-of-fit with data by 3.7% and 0.6% using GFDL and ERSEM outputs, respectively. In addition, the projected rate of latitudinal shift of pelagic species is slower when considering interactions between species. Our approach addresses a recognised gap in bioclimate envelope models for modelling considering climate change, and has the advantage that it can be applied on ecosystem, sea-basin and global scales without detailed information on dietary interactions among species.

Introduction

Climate change is expected to increasingly affect ocean conditions, including temperature, salinity, ice coverage, currents, oxygen level, acidity, and consequently distribution, productivity and abundance of marine species, including fishery resources (Behrenfeld *et al.* 2006; Brander 2007; Perry *et al.* 2005; Pörtner 2010; Simpson *et al.* 2011). Over a range of greenhouse gas emission scenarios (IPCC 2007), changes in the marine environment are expected to be more rapid in the 21st century with implications for dependent communities and industries (Roessig *et al.* 2004; Lam *et al*. 2012; Merino *et al*. 2012). Ecological interactions in marine ecosystems are complex, making it difficult to extrapolate from studies of individuals and populations to community or ecosystem level (Walther *et al.* 2002). It is also known that these interactions can result in additive, antagonistic and synergistic responses to climate and fishing forcing (Griffith *et al.* 2011).

A range of modelling approaches has been developed to predict the potential effects of future climate change on species distributions and abundance (Stock *et al*. 2011). One class of models, species-based bioclimate envelope models, have been used to predict redistribution of both terrestrial and aquatic species (Pearson and Dawson 2003; Jones *et al*. 2012). The Dynamic Bioclimate Envelope Model (DBEM) developed by Cheung *et al*. (2008a, 2008b, 2009, 2011) projects changes in marine species distribution, abundance and body size with explicit consideration of population dynamics, dispersal (larval and adult) and ecophysiology (Cheung *et al*. 2008a, 2008b, 2009, 2011, 2012). Projections suggest that there will be a high rate of species invasions in high-latitude regions and a potential high rate of local extinction in the tropics and semi-enclosed seas in the 21st century (Cheung *et al*. 2009). Moreover, as a result of predicted changes in range and primary productivity, Cheung *et al*. (2010) project that maximum catch potential of exploited species is expected to decrease in the tropics and to rise in high latitudes. Consideration of the effects of ocean de-oxygenation and ocean acidification may result in further decreases in projected catch, despite considerable uncertainties (Cheung *et al*. 2011). However, these projections do not account for the effects of species interactions on redistribution and abundance, which introduces a source of structural uncertainty (Cheung *et al*. 2010).

Rates of primary production and transfer efficiency influence production and biomass along and at the top of ecological food webs. Size spectrum theory accounts for energy transfer from primary producers to animals of progressively larger body size and are an alternative to describe changes in biomass and production with body size (Sheldon *et al.* 1977; Dickie *et al.* 1987). Size spectrum theory has been developed and applied to predict potential biomass, production and size structure of fish in the world's oceans from primary production (Jennings *et al.* 2008), and to the responses of fish communities to fishing and climate change (Blanchard *et al.* 2011). These size spectrum models are not resolved taxonomically, and this limits their value in assessing climate change implications for fisheries, as the species composition as well as the quantity of potential landings is an important consideration for the fishing industry and management agencies.

Here, we combine the strengths of the DBEM (i.e., focus on identified species) and the size spectrum model (i.e., focus on trophic interactions) to predict spatial and temporal changes in species abundance and distribution in response to predicted future changes in temperature and primary production. Forty-eight of the most abundant and commercially important marine fishes in the North Atlantic, here defined as coming from Food and Agriculture Organization (FAO) statistical area 27, are included. The size spectrum is used to determine resource limits in a particular geographical area of the ocean and these limits, along with habitat suitability for a given species, determine the biomass of that species that can be supported in this area.

Methods

A modelling approach that integrates the species-based DBEM model with the size spectrum approach, hereafter called size-spectrum DBEM (SS-DBEM) was developed. The SS-DBEM: (1) estimates potential biomass supported by the system, (2) predicts habitat suitability and (3) models competition. Predictions from the SS-DBEM are then compared with a DBEM model that does not incorporate species interactions (NSI-DBEM, where NSI denotes no species interactions).

Potential biomass supported at each body size class

The size-spectrum is described as a log-log relationship between abundance and body size. The slope and height of the spectrum are determined by the energy transfer efficiency of the system and its primary production defining the maximum total abundance of individuals from all species that can be supported in any defined body size class.

Since predator-prey mass ratios and transfer efficiencies in marine food chains do not depend on the mean rate of primary production or mean temperature, less energy is transferred to consumers of a given body size when food webs are supported by smaller primary producers (Barnes *et al.* 2010). Much of the variation in the body size distribution of primary producers depends on the absolute rate of primary production, with picoplankton, the smallest phytoplankton, dominating when primary production is low (Agawin *et al.* 2000) and the mid-point size of phytoplankton decreasing with decreasing rates of primary production (Barnes *et al.* 2011). To account for this, the position of the median body mass class for phytoplankton was calculated as:

$$\mathrm{m} = [(-6.1 \cdot \mathrm{P_s}) - 8.25]/\log_{10}(2) \quad (1)$$

where P_s is the predicted contribution of picophytoplankton net production to total Net Primary Production (PP) as calculated using the empirical equation

$$\mathrm{P_s} = [(12.19 \log \mathrm{PP}) + 37.248]/100 \quad (2)$$

derived from the data of Agawin *et al.* (2000) by Jennings *et al.* (2008).

Once the median body mass class of phytoplankton was defined, we calculated the consumer biomass at body size following the methods described in Jennings *et al.* (2008). The same assumptions were adopted about predator-prey size preferences and transfer efficiency as in Jennings *et al.* (2008), but discretized the spectrum using a $\log_2$ series of body mass from 2^1 to 2^{19} g.

Habitat suitability

The development of the dynamic bioclimate envelope model within the SS-DBEM was based on the approach of Cheung *et al.* (2008a, 2008b, 2009, 2011, 2012). The NSI-DBEM defines the relative preferences of the modelled species for temperature and other environmental

variable based on the relationship between the current distributions and gridded environmental data. The current (representing 1970 – 2000) distribution of relative abundance of the modelled marine species on a ½ x ½ degree latitude-longitude grid map of the world ocean, are predicted using the *Sea Around Us* project algorithm (Close *et al*. 2006). Environmental variables incorporated into the NSI-DBEM include sea surface temperature, sea bottom temperature, coastal upwelling, salinity, sea-ice extent and habitat type (Cheung *et al.* 2011). First, NSI-DBEM calculates changes in growth and other life history traits in response to changes in temperature and oxygen concentration based on algorithms derived from growth and metabolic functions and empirical equations (Cheung *et al*. 2011, 2012). Second, NSI-DBEM predicts size-frequency distributions for each species in each spatial cell using a size-structured 'per recruit' model. Finally, the model simulates spatial and temporal changes in relative abundance within a cell based on carrying capacity of a cell, population growth, larval dispersal and adult migration (Cheung *et al.* 2008b, 2011).

Competition

A new algorithm was developed to describe resource competition between different species co-occurring in a cell by comparing the energy (in biomass) that can be supported in the cell (estimated with the SS model) with the energy demanded by the species predicted to inhabit the given cell (estimated with the NSI model). The algorithm comprises two stages: (1) an initialization stage where competition parameters are estimated; and, (2) a recurrent stage where the competition parameters are used to resolve conflicts between energy (biomass) demands and biomass that can be supported.

First stage

The model uses the NSI-DBEM approach to establish an initial distribution for each species assuming that predicted habitat suitability is a proxy for the distribution of relative abundance of a given species. Thus, multiplying the initial relative biomass by the estimated absolute biomass from empirical data, initial species distribution is expressed in terms of absolute biomass in each cell. This allows the calculation of total biomass of biota by adding predicted distributions across species. Since biomass estimates from survey data are not available for some of the species considered (Table 1), the initial biomass estimates were approximated by the predicted unexploited biomass (B_∞) from maximum reported fisheries catch (MC) since 1950 and an estimate of the intrinsic growth rate (r) of the population (Schaefer 1954):

$$B_\infty = MSY \cdot 4/r \quad (3)$$

where, MSY is the maximum sustainable yield. Strengths and weaknesses of this assumption are documented by Froese *et al.* (2012). However, this determines only an initialization point for the model to differentiate between abundant and rare species. Maximum catch was calculated from the algorithm documented in Cheung *et al*. (2008) while estimated *r* values, based on an empirical equation that is dependent on asymptotic length of the species, were obtained from FishBase (www.fishbase.org). Although this is an approximation and not as reliable as estimates of biomass in the sea, we consider that despite some significant

variability, biomass estimates from maximum catch data and aggregated stock assessments (Table 1) are significantly correlated for the considered species (Fig. 1).

The initial absolute biomass estimates, based on habitat suitability in the cells where they are distributed (Fig. 2), are used to generate a matrix of species energy (biomass) demand. Matrix elements define the proportion of total energy, available to a species at each habitat suitability and size class. The amount of energy is determined by the average proportion of energy that a species gets in cells with the same habitat suitability.

Energy demanded (E_D) by a species in a cell is compared with the total biomass or energy (E_S) that can be supported in the cell (see Table 2 for a summary of abbreviations). E_D is determined by the NSI-DBEM, whereas the E_S is determined by the SS model. Thus, the average proportion of energy that a species demands in cells of same habitat suitability can be calculated:

$$\text{resouces}_{\text{Spp,Suit,Size}} = \frac{\text{E\_D}^{\text{Suit}}_{\text{Spp,W,i}}}{\text{E\_S}_{\text{W,i}}} \quad (4)$$

To convert from biomass (B) distribution to abundance (N) and *vice versa*, the mean body mass (W) at each size class (*i*) is used:

$$B = \sum_{i=1}^{n} N_i \times W_i \quad (5)$$

where, n is the number of size class considered in the model. The initial habitat suitability value is converted using a square root data transformation to ensure a balanced distribution of the cells across the habitat suitability classes and then normalized to a range from 0 to 1 relative to minimum and maximum value of habitat suitability for each species. The model then groups habitat suitability into six classes (bins) of values: 0 - 0.3, >0.3 - 0.4, >0.4 - 0.5, >0.5 - 0.6, >0.6 - 0.7 and >0.7 - 1. The use of discretized bins of habitat suitability, a non-parametric methodology, does not require the specification and estimation of particularly distribution functions and is considered a more computationally efficient method (Fayyad and Irani 1993, Dougherty *et al.* 1995). The effects of potential error from such discretization is minimized here by using a squared root transformation of the predicted habitat suitability, a low number of bins and the choice of the bins boundaries (Uusitalo 2007; Fernandes *et al.* 2010).

Available energy in a size class which is not demanded by the modelled species was assigned to a group called ‘other groups’. This group has its own resource allocation matrix based on the average habitat suitability of the modelled species. Only cells with a minimum number of modelled species are considered to compute the ‘others group’ matrix, with the minimum species number being the square root of the number of species modelled. This formulation allows the inclusion of resource demand from species that are not explicitly modelled.

Second stage

Abundance of each species in each cell was predicted based on the algorithm used by the NSI-DBEM. The model runs in an annual time-step for bottom-dweller (demersal) species and two seasonal time-steps (summer and winter) for species in the water-column (pelagic). For each species, the energy demands are compared with energy demands of other species co-occurring in the same cell (Table 3). If the energy demand by all organisms in the cell exceeds the energy available, and then the available energy was allocated to each species in proportion to their energy demands within the cell. If the energy demanded by all the species is lower than the energy available, the surplus energy was allocated according to the proportional energy demand of the species present. To represent population growth that is limited by factors other than available energy, the rate that energy can actually be assimilated by a species is limited:

$$\mathrm{res\_op}_{\mathrm{Spp,Suit,W}} = \frac{2 \cdot \mathrm{std.dev}(\mathrm{E\_D}^{\mathrm{Suit}})}{\mathrm{mean}(\mathrm{E\_D}^{\mathrm{Suit}})} \quad (6)$$

Where, $\mathrm{E\_D}^{\mathrm{Suit}}$ denotes the energy demanded in all the cells in each bin of habitat suitability. Therefore, the amount of additional energy that can be taken by the species is limited by two times the standard deviation (std.dev) of energy that each species gets in the initial distribution at each habitat suitability bin. Any energy that is left after these allocation is assumed to be used by the *Others* group.

Model testing

The results from the model that includes competition were compared with results from the NSI-DBEM and "empirical" time series of abundance data from fish stock assessments for the Northeast Atlantic (FAO area 27), as extracted from the RAM Legacy Stock Assessment Database (Ricard *et al.* 2011; http://ramlegacy.marinebiodiversity.ca/) and ICES Stock Summary Database (http://www.ices.dk). To compare projected changes with observations, both datasets are normalized by dividing them by their mean value. While the models were applied to a set of 48 fish species, comparison with empirical data were conducted for 24 species with available data from the above assessments datasets (Table 1). The output of the DBEM models are compared with the "empirical" time series values for each species observing the distribution of absolute error (AE):

$$\mathrm{AE} = \left|\mathrm{p_j}\text{-}\mathrm{x_j}\right| \quad (7)$$

where, p is the total biomass predicted in a DBEM model in a particular year for a species, and x is the total biomass from the assessments. The comparison was done for the years with available assessment data for all the 24 species considered. To compare between the performance of SS-DBEM and NSI-DBEM, Percent Reduction in Error (PRE) was calculated (Hagle and Glen 1992; Fernandes *et al.* 2009), but weighted by the maximum catch of each species (WPRE):

$$\mathrm{WPRE} = \frac{1}{\sum_{k=1}^{l} \mathrm{MaxCatch}_k} \sum_{k=1}^{l} \left[\frac{100(\mathrm{AENSI_k}\text{-}\mathrm{AESS_k})}{\mathrm{AENSI_k}}\right] \cdot \mathrm{MaxCatch}_k \quad (8)$$

where AENSI is the absolute error in the NSI-DBEM model, AESS is the absolute error in the SS-DBEM model, k the number of species and MaxCatch the maximum catch of the species.

These models were also compared with empirical data in describing latitudinal and depth centroid shifts of species in response to climate change (Dulvy *et al.* 2008; Cheung *et al.* 2011). Distribution centroid (DC_t) for each year (t) was calculated as:

$$DC_t = \frac{\sum_i^n B_{t,i} \cdot A_i \cdot Lat_i}{\sum_i^n B_{t,i} \cdot A_i}; \quad (9)$$

where, B_i is the predicted relative abundance in cell *i*, *A* is the area of the cell, *Lat* is the latitude at the centre of the cell and *n* is the total number of cells where the species was predicted to occur. We calculated the rate of range shift as the slope of a fitted linear regression between the distribution centroid of the species and time. We expressed latitudinal range shift (*LS*) as poleward shift in distance from:

$$LS = DS \cdot \pi/180 \cdot 6378.2; \quad (10)$$

where *DS* is the distribution shift in degree latitude per year.

The models were run for a time-frame of 35 years, from 1970 to 2004 with environmental forcing predicted from two modelling systems: (1) the National Oceanographic and Atmospheric Administration (NOAA) Geophysical Fluid Dynamic Laboratory Earth System Model (ESM) 2.1(GFDL) and (2) the European Regional Seas Ecosystem Model (ERSEM). GFDL ESM2.1 is a global atmosphere-ocean general circulation model (Delworth *et al.* 2006) coupled to a marine biogeochemistry model (TOPAZ; Dunne *et al.* 2010) which includes major nutrients and three phytoplankton functional groups with variable stoichiometry. For the GFDL hindcast simulations (Henson *et al.* 2010), air temperature and incoming fluxes of wind stress, freshwater, shortwave and longwave radiation are prescribed as boundary conditions from the CORE- version 2 reanalysis effort (Large and Yeager 2009). ERSEM is a biogeochemical model that uses the functional-groups approach which decouples carbon and nutrient dynamics and comprises four phytoplankton and three zooplankton functional groups (Blackford *et al.* 2004).Data from two different configurations of ERSEM were applied here: on the global scale a hindcast of the NEMO-ERSEM model forced with DFS 4.1 reanalysis for the atmosphere (Dunne *et al*. 2010) and on the regional scale a hindcast of the POLCOMS-ERSEM model for the NW-European shelf forced with ERA 40 reanalysis (extended with operational ECMWF reanalysis until 2004) for the atmosphere and global ocean reanalysis for the open ocean boundaries (more details on the configuration can be found in Holt *et al.* 2012; Artioli *et al.* 2012). The data from this global model was overlapped by the data from a regional model of the North Sea area.

Results and discussion

Comparing SS-DBEM with NSI-DBEM

Predicted biomasses from SS-DBEM were generally lower than those projected from NSI-DBEM (Fig. 3). The reason is that a limit on the energy available from primary producers plays an important role in limiting species' biomass in SS-DBEM but not in NSI-DBEM, where species' carrying capacity depends mainly on the habitat suitability of the cell. The chosen energy based competition does not model the real species interactions. The advantage is easy parameterisation and the disadvantage is that interactions are not specified (e.g. no diet matrix). However, a diet matrix is very hard to implement and will part from assumptions such that a species will not change its diet to an opportunistic strategy. The proposed approach has the advantage that is also able to new situations such as new predators invading an area and interacting with species for first time. An acceptable balance between abstraction and detail is needed to address questions about large-scale redistribution and build scenario of what-if kind (Metcalfe *et al.* 2012).

Outputs from SS-DBEM explain more of the variation in biomass estimated from stock assessments (FAO area 27) than those from the NSI-DBEM. The error weighted by maximum catch predicted across species from SS-DBEM against empirical data is 3.7% lower than those predicted from NSI-DBEM using GFDL environmental forcing data and 0.6% lower using ERSEM data. GFDL might be more accurate (Fig. 4) for the time period considered since the model run was forced by re-analysis data such as surface temperature and wind fields, which is not the case for ERSEM. However, the differences in mean absolute error are not significant and might not hold when the models are used for forecasting. Finally, a lower variance in the absolute error in SS-DBEM with respect to NSI-DBEM model (Fig. 4) is indicative of a higher precision of simulated biomass from SS-DBEM (Taylor 1999). All this supports also the assumption that with better primary production estimates available the proposed modelling approach can potentially be a great advance over models without any kind species interactions mechanism.

Distribution shift

Both NSI-DBEM and SS-DBEM projected poleward latitudinal shift of species distributions (Fig. 5), and the projected shifts are generally consistent between simulations forced by the two sets of Earth System Model outputs (Table 4). In addition, the projected shift of pelagic species by the model with interactions is consistently lower than if no interactions are considered (Table 4). However, to the best of our knowledge there is still no study based on observational data that confirms or denies this result. With ERSEM forcing, the median projected rates of pole ward shift are 63.5 km and 54.9 km over 35 years, or 18.1 and 15.7 km decade^{-1}, from NSI-DBEM and SS-DBEM respectively. All sets of simulations show a higher rate of range shift for pelagic species than bottom dwelling species. A reduction in the expected geographical shift of particular populations as a result of ecological interactions is consistent with the perception of compensatory ecological processes (Frank *et al.* 2011). In

terms of depth shift, in general, the results show a shift to shallower waters at a rate ranging from 0.4 to 8.7 m decade^{-1}. The shift in depth is also dependent on the spatial domain considered. For example, for demersal species in FAO Area 27, outputs from SS-DBEM driven by ERSEM data project a shift to deeper waters of 1.3 m decade^{-1}. However, when we consider North Sea only, the projected shift to deeper waters is higher at 5.7 m decade^{-1}.

The projected rates of shifts from the SS-DBEM are consistent with observations. Specifically, Perry *et al.* (2005) projected a mean rate of latitudinal shift of 22 km decade^{-1} from 1980 to 2004 in the North Sea for six fish species. Comparable rates of shift (between 18.5 and 18.8 km decade^{-1}) are projected here for the four of these species (bib, blue whiting, Norway pout and Witch). Also, Dulvy *et al.* (2008) estimated that bottom dwelling species were moving into deeper waters at an average rate of 3.1 m decade^{-1} from 1980 to 2004 (19 species out of 28 species are common between this study and Dulvy *et al.* 2008), a little slower that our prediction of 5.7 m decade^{-1}. These direct comparisons between predicted and observed shifts need to be interpreted with caution because of the differences in the species included and spatial domain. In addition, these are projections are of full species distribution, not stocks. This is because the data about species life history needed to produce such projections is available at species level and not at the level of specific stocks. Therefore, the trend or shift of certain species has not to be consistent across all the stocks (Petitgas *et al.* 2012).

Maximum catch

The predicted maximum catch by the both DBEM models (SS and NSI) follows a similar trend to the empirical total catches for the 1970 to 2004 time period in the ICES areas (Fig. 6). The empirical catch data is the result of aggregating all the catches reported in ICES areas as collected in the Eurostat/ICES database on catch statistics - ICES 2011, Copenhagen (http://www.ices.dk). The predicted maximum catch is based on the aggregation of the potential catch of the 48 modelled species in ICES areas. This can mean that despite inaccuracies in some species, the models are able to reproduce observed fish productivity in the North East Atlantic.

This estimate is based on the sum of the predictions for each species. Catch predicted from SS and NSI approaches show similar pattern when the most abundant and commercially important species are aggregated. Incorporating species interactions in the model does not reduce the total catch predicted. Further work will focus on examining the effects of different modelling approaches on catch predicted for specific species, areas (e.g. ICES areas) or community size class.

Model uncertainty

Earth System Models are known to systematically project lower primary production over continental shelves, a consequence of their limited spatial resolution. This effect cannot be corrected directly. Therefore, the output of the model has to be considered in terms of relative change over time and space. Efforts to understand and produce for a more accurate primary production projections are being made (Holt *et al.* 2012; Krause-Jensen *et al.* 2012).

Meanwhile, available projections can be used to study the interactions between species and evaluate how species interactions may affect changes in distribution.

A main assumption of size-spectrum component of the model is that size spectrum function for a given community is considered to be a linear relationship between log-abundance and log-size classes. Such assumption is made mainly for computational performance. In reality, such assumption may be violated as species shift their distribution or when primary productivity changes, resulting in non-linearity in the size spectrum. However, our model simulations show that such violation of assumption is rare (in less than 5% of cells), except for a few species (violation in 80 – 100% of the cells). However, in all the species the break or drop is consistently a small percentage of the abundance in the cell (an average of 0.034 % of abundance decrease), indicating that the assumption has limited effect on the projections.

The use of the new model with species interactions improves the forecasting power over previous versions of the model with benefits in terms of improving total catch potential estimation. We applied theoretical mechanism and empirical data to model trophic interactions. Although the modelling approach does not incorporated the full range of complexity of interactions between species in marine food-webs, the ease of parameterization allows the model to be applicable to large number of species in most part of the global ocean to develop scenarios of large-scale shift in species distribution and fisheries catch (Cheung *et al.* 2010; Metcalfe *et al.* 2012). A multi-model approach with projections from model with different complexity, such as the analysis in this study, would facilitate the exploration of model uncertainties in developing scenarios of biological responses to climate change and their socio-economic implications (Jones *et al.* 2012).

References

Agawin NSR, Duarte CM, Agust S. (2000) Nutrient and temperature control of the contribution of picoplankton to phytoplankton biomass and production. *Limnology Oceanography* 45, 591–600.

Artioli Y, Blackford JC, Butenschön M, *et al.* (2012) The carbonate system in the North Sea: Sensitivity and model validation. *Journal of Marine Systems* 102-104, 1-13.

Barnes C, Maxwell D, Reuman DC, Jennings S. (2010) Global patterns in predator-prey size relationships reveal size dependency of trophic transfer efficiency. *Ecology* 91 (1), 222-232.

Barnes C, Irigoien X, De Oliveira JA, Maxwell D, Jennings S (2011) Predicting marine phytoplankton community size structure from empirical relationships with remotely sensed variables. *Journal of Plankton Research* 33 (1), 13-24.

Behrenfeld MJ, O'Malley RT, Siegel DA, McClain CR, Sarmiento JL, Feldman GC, Milligan AJ, Falkowski PG, Letelier RM, Boss ES (2006) Climate-driven trends in contemporary ocean productivity. *Nature* 444, 752-755.

Blackford JC, Allen JI, Gilbert FJ (2004) Ecosystem dynamics at six contrasting sites: a generic modelling study. *Journal of Marine Systems* 52 (1), 191-215.

Blanchard JL, Law R, Castle MD, Jennings S (2011) Coupled energy pathways and the resilience of size-structured food webs. *Theoretical Ecology* 4 (3), 1-12.

Brander KM (2007) Global fish production and climate change. *Proceedings of the National Academy of Sciences* 104 (50), 19709-19714.

Cheung WWL, Close C, Lam V, Watson R, Pauly D (2008a) Application of macroecological theory to predict effects on climate change on global fisheries potential. *Marine Ecology Progress Series* 365, 187-197.

Cheung WWL, Lam VWY, Pauly D (2008b) Modelling Present and Climate-Shifted Distribution of Marine Fishes and Invertebrates. Fisheries Centre Research Report 16(3), University of British Columbia, Vancouver, Canada.

Cheung WWL, Close C, Kearney K, Lam V, Sarmiento J, Watson R, Pauly D (2009) Projections of global marine biodiversity impacts under climate change scenarios. *Fish and Fisheries* 10, 235–251.

Cheung WWL, Dunne J, Sarmiento JL, Pauly D (2011) Integrating ecophysiology and plankton dynamics into projected maximum fisheries catch potential under climate change in the Northeast Atlantic. *ICES Journal of Marine Science* 68 (6), 1008-1018.

Cheung WWL, Sarmiento JL, Dunne J, Frolicher T, Lam V, Palmoares MLD, Watson R, Pauly D (2012) Shrinking of fishes exacerbates impacts of global ocean changes on marine ecosystems. *Nature Climate Change*, Change10.1038/nclimate1691.

Close C, Cheung WWL, Hodgson S, Lam V, Watson R, Pauly D (2006) Distribution ranges of commercial fishes and invertebrates. In: Palomares, M. L. D., Stergiou, K. I., Pauly, D. (eds). Fishes in Databases and Ecosystems. Fisheries Centre Research Reports 14 (4). Fisheries Centre, University of British Columbia, Vancouver, p 27-37.

Delworth TL, Rosati A, Stouffer RJ, *et al.* (2006) GFDL's CM2 global coupled climate models. part I: formulation and simulation characteristics. *Journal of Climate* 19, 643-674.

Dickie LM, Kerr SR, Boudreau PR (1987) Size-dependent processes underlying regularities in ecosystem structure. *Ecological Monographs* 57, 233-250.

Dougherty J, Kohavi R, Sahami M (1995) Supervised and unsupervised discretization of continuous features. In: A. Prieditis and S. Russell, (eds.), Proceedings of International Conference on Machine Learning. Morgan Kaufmann, San Francisco, CA, USA, pp. 194-202.

Dulvy NK, Rogers SI, Jennings S, *et al.* (2008) Climate change and deepening of the North Sea fish assemblage: a biotic indicator of warming seas. *Journal of Applied Ecology* 45, 1029–1039.

Dunne JP, Gnanadesikan A, Sarmiento JL, Slater RD (2010) Technical description of the prototype version (v0) of tracers of phytoplankton with allometric zooplankton (TOPAZ) ocean biogeochemical model as used in the Princeton IFMIP model. *Biogeosciences* 7 (Suppl.), 3593.

Fayyad U, Irani K(1993) Multi-interval discretization of continuous-valued attributes for classification learning. In: Proceedings of the Thirteenth International Joint Conference on Artificial Intelligence. pp. 1022-1027.

Fernandes JA, Irigoien X, Boyra G, Lozano JA, Inza I (2009) Optimizing the number of classes in automated zooplankton classification. *Journal of Plankton Research* 31 (1), 19-29.

Fernandes JA, Irigoien X, Goikoetxea N, Lozano JA, Inza I, Pérez A, Bode A (2010) Fish recruitment prediction, using robust supervised classification methods. *Ecological Modelling* 221 (2), 338-352.

Frank KT, Petrie B, Fisher JA, Leggett WC (2011) Transient dynamics of an altered large marine ecosystem. *Nature* 477 (7362), 86-89.

Froese R, Zeller D, Kleisner K, Pauly D (2012) What catch data can tell us about the status of global fisheries. *Marine biology* 159 (6), 1283-1292.

Griffith GP, Fulton EA, Richardson AJ (2011) Effects of fishing and acidification-related benthic mortality on the southeast Australian marine ecosystem. *Global Change Biology*, 17 (10), 3058-3074.

Hagle TM, Glen EM (1992) Goodness-of-fit measures for Probit and Logit. *American Journal of Political Science* 36 (3), 762-784.

Henson SA, SarmientoJL, Dunne JP, *et al.* (2010) Detection of anthropogenic climate change in satellite records of ocean chlorophyll and productivity. *Biogeosciences* 7, 621-640.

Holt J, Butenschön M, Wakelin SL, Artioli Y, Allen JI (2012) Oceanic controls on the primary production of the northwest European continental shelf: model experiments under recent past conditions and a potential future scenario. *Biogeosciences* 9 (1), 97-117.

IPCC (2007) Summary for policymakers. In Climate Change 2007: the Physical Science Basis. Working Group I Contribution to the Fourth Assessment Report of the IPCC, pp. 1–18. Ed. by S. Solomon, D., Qin, M., Manning, Z., Chen, M., Marquis, K. B., *et al.* Cambridge University Press, Cambridge.

Jennings S, Mélin F, Blanchard JL, Forster RM, Dulvy NK, Wilson RW (2008) Global-scale predictions of community and ecosystem properties from simple ecological theory. *Proceedings of the Royal Society B: Biological Sciences* 275 (1641), 1375-1383.

Jones MC, Dye SR, Pinnegar JK, *et al.* (2012) Modelling commercial fish distributions: Prediction and assessment using different approaches. *Ecological Modelling* 225, 133-145.

Krause-Jensen D, Markager S, Dalsgaard T (2012) Benthic and Pelagic Primary Production in Different Nutrient Regimes. *Estuaries and coasts* 35 (2), 527-545.

Lam VW, Cheung WWL, Swartz W, Sumaila UR (2012) Climate change impacts on fisheries in West Africa: implications for economic, food and nutritional security. *African Journal of Marine Science* 34 (1), 103-117.

Large W, Yeager S (2009) The global climatology of an interannually varying air-sea flux data set. *Climate Dynamics* 33, 341-364.

Metcalfe JD, Le Quesne WJF, Cheung WWL, Righton DA (2012) Conservation physiology for applied management of marine fish: perspectives on the role and value of telemetry. *Philosophical Transactions of the Royal Society B* 367, 1746-1756.

Merino G, Barange M, Blanchard JL, et al. (2012) Can marine fisheries and aquaculture meet fish demand from a growing human population in a changing climate? *Global Environmental Change* 22 (4), 795-806.

Pearson RG, Dawson TP (2003) Predicting the impacts of climate change on the distribution of species: are bioclimate envelope models useful? *Global Ecology and Biogeography* 12, 361-371.

Perry AL, Low PJ, Ellis JR, Reynolds JD (2005) Climate change and distribution shifts in marine fishes. *Science* 308, 1912-1915.

Pörtner HO (2010) Oxygen- and capacity-limitation of thermal tolerance: a matrix for integrating climate-related stressor effects in marine ecosystems. *Journal of Experimental Biology* 213, 881-893.

Petitgas P, Alheit J, Peck MA, *et al.* (2012) Anchovy population expansion in the North Sea. *Marine Ecology-progress Series* 444, 1-13.

Ricard D, Minto C, Jensen OP, Baum JK (2012) Evaluating the knowledge base and status of commercially exploited marine species with the RAM Legacy Stock Assessment Database. *Fish and Fisheries* 13 (4), 380-398.

Roessig JM, Woodley CM, Cech JJ, Hansen LJ (2004) Effects of global climate change on marine and estuarine fishes and fisheries. *Reviews in Fish Biology and Fisheries* 14, 251-275.

Schaefer MB (1954) Some aspects of the dynamics of populations important to the management of the commercial marine fisheries. *Bulletin of the Inter-American Tropical Tuna Commission* 1, 25-56.

Sheldon RW, Sutcliffe WH, Paranjape MA (1977) Structure of pelagic food chain and relationship between plankton and fish production. *Journal of the Fisheries Research Board of Canada* 34, 2344-2355.

Simpson SD, Jennings S, Johnson MP, Blanchard JL, Schön PJ, Sims DW, Genner MJ (2011) Continental shelf-wide response of a fish assemblage to rapid warming of the sea. *Current Biology* 21 (18), 1565-1570.

Stock CA, Alexander MA, Bond NA, *et al.* (2011) On the use of IPCC-class models to assess the impact of climate on living marine resources. *Progress in Oceanography* 88 (1-4), 1-27.

Taylor JR (1999) An introduction to error analysis: The Study of Uncertainties in Physical Measurements. University Science Books. pp. 128–129

Uusitalo L (2007) Advantages and challenges of Bayesian networks in environmental modelling. *Ecological Modelling* 203, 312-318.

Walther GR, Post E, Convey P, *et al.* (2002) Ecological responses to recent climate change. *Nature* 416 (6879), 389-395.

Tables

Table 1. List of modelled fish species. Species with biomass assessment are marked in the last column. In the last column, stocks that have been aggregated for the species from RAM database (STOCKID) are listed in capital letters. For some stocks not recorded in the RAM database, ICES Stock Summary Database was used (listed with no-capital letters).

Common name	Scientific name	Type	Stocks
Albacore	*Thunnus alalunga*	Pelagic	ALBANATL.
American plaice/long rough dab	*Hippoglossoides platessoides*	Demersal	
Angler	*Lophius piscatorius*	Demersal	
Atlantic cod	*Gadus morhua*	Demersal	CODNEAR, CODBA2224, CODBA2532, CODVIa, CODIS, CODICE, CODNS and CODKAT.
Atlantic herring	*Clupea harengus*	Pelagic	HERRIsum, HERRNS, HERRVIa, ERRVIaVIIbc, HERR2224IIIa, HERR2532, HERR30, HERRRIGA, HERRNIRS, HERRNWATLC, HERR4VWX, HERR4RFA, HERR4RSP, HERR4TFA, HERR4TSP, HERR31,her-vian, her-noss andher-vasu
Atlantic horse mackerel	*Trachurus trachurus*	Pelagic	hom-west.
Atlantic mackerel	*Scomber scombrus*	Pelagic	MACKNEICES.
Baltic sprat	*Sprattus sprattus*	Pelagic	SPRAT22-32.
Blue whiting	*Micromesistius poutassou*	Pelagic	whb-comb.
Boarfish	*Capros aper*	Demersal	
Capelin	*Mallotus villosus*	Pelagic	CAPEICE and CAPENOR.
Common sole	*Solea solea*	Demersal	SOLENS, SOLEVIId, SOLEIS, SOLEIIIa, SOLEVIIe, SOLECS, and SOLEVIII.
Cuckoo ray	*Leucoraja naevus*	Demersal	
Dab	*Limanda limanda*	Demersal	
European anchovy	*Engraulis encrasicolus*	Pelagic	ANCHOBAYB.
European hake	*Merluccius merluccius*	Demersal	HAKESOTH and HAKENRTN.
European pilchard	*Sardina pilchardus*	Pelagic	sar-soth.
European plaice	*Pleuronectes platessus*	Demersal	PLAIC7d, PLAICIIIa, PLAICNS, PLAICIS, PLAICECHW and PLAICCELT.
European sprat	*Sprattus sprattus*	Pelagic	SPRATNS.
Flounder	*Platichthys flesus*	Demersal	
Fourbeard rockling	*Enchelyopus cimbrius*	Demersal	
Fourspotted megrim	*Lepidorhombus boscii*	Demersal	mgb-8c9a.
Greenland halibut	*Reinhardtius hippoglossoides*	Demersal	GHALNEAR, GHALBSAI and GHAL23KLMNO.

Haddock	*Melanogrammus aeglefinus*	Demersal	HAD4X5Y, HAD5Y, HAD5Zejm, HADICE, HADNEAR, HADFAPL, HADNS-IIIa, HADVIa, HADVIIb-k, HADROCK and HADGB.
John dory	*Zeus faber*	Demersal	
Lemon sole	*Microstomus kitt*	Demersal	
Ling	*Molva molva*	Demersal	
Megrim	*Lepidorhombus whiffiagonis*	Demersal	mgw-8c9a.
Northern bluefin tuna	*Thunnus thynnus*	Pelagic	ATBTUNAEATL and ATBTUNAWATL.
Norway pout	*Trisopterus esmarkii*	Demersal	nop-34.
Golden Redfish	*Sebastes norvegicus*	Demersal	GOLDREDNEAR.
Pearlsides	*Maurolicus muelleri*	Pelagic	
Piked dogfish/ Spurdog	*Squalus acanthias*	Demersal	
Pollack	*Pollachius pollachius*	Demersal	
Poor cod	*Trisopterus minutus*	Demersal	
Pouting / Bib	*Trisopterus luscus*	Demersal	
Red bandfish	*Cepola macrophthalma*	Demersal	
Saithe / Pollock	*Pollachius virens*	Demersal	POLL5YZ, POLLNEAR, POLLFAPL, POLL4X5YZ and POLLNS-VI-IIIa.
Smallspottedcatshark	*Scyliorhinus canicula*	Demersal	
Splendid alfonsino	*Beryx splendens*	Demersal	
Spotted ray	*Raja montagui*	Demersal	
Striped red mullet	*Mullus surmuletus*	Demersal	
Thickback sole	*Microchirus variegatus*	Demersal	
Thornback ray	*Raja clavata*	Demersal	
Tub gurnard	*Chelidonichthys lucerna*	Demersal	
Tusk/ Torsk / Cusk	*Brosme brosme*	Demersal	CUSK4X.
Whiting	*Merlangius merlangus*	Demersal	WHITNS-VIId-IIIa, WHITVIa and WHITVIIek.
Witch	*Glyptocephalus cynoglossus*	Demersal	

Table 2. Summary of abbreviations.

Abbreviation	Description	Details
I	Index of cell	From 0 to 250200
Spp	Index of species	From 0 to 16 species
Suit	Index of the habitat suitability bin	Between 0 and 1, 4 bins
W	Index of the size spectrum	21 log2 classes from 2^{-1} to 2^{19}
$res_{Spp,Suit,W}$	Proportion resources atmatrix of energy demand	See Eq. 4
$res^{Suit}_{Spp,W,i}$	Actual proportion of resources by competition	See Table 3
$E\_S_{size,i}$	Total biomass supported in a cell	Calculated from Primary production
$E\_C^{\boldsymbol{Suit}}_{Spp,W,i}$	Biomass by competition	$res^{Suit}_{Spp,W,i} \cdot E\_S$
$E\_D^{\boldsymbol{Suit}}_{Spp,W,i}$	Biomass demanded	Calculated at each yearly shift
$TotalRes_{W,i}$	Total proportion of resources demanded	$\sum_{Spp} res^{Suit}_{Spp,W,i}$
$Res\_op_{Spp,Suit,W}$	Proportion of resources by opportunity	See Eq. 6

Table 3.Pseudocode of the competition algorithm which resolves conflicts between the energy demanded and supported.

Competition algorithm pseudocode
1: Calculate $E\_C^{\boldsymbol{Suit}}_{Spp,W,i} = res_{Spp,Suit,W} * E\_S$
2: $E\_C^{\boldsymbol{Suit}}_{Spp,W,i} > E\_D^{\boldsymbol{Suit}}_{Spp,W,i}$
3: Then % $res^{Suit}_{Spp,Size,i} = E\_D^{\boldsymbol{Suit}}_{Spp,W,i} / E\_S_{W,i}$
5: If $TotalRes_{W,i} < 1$ Then $res^{Suit}_{Spp,W,i}$ from matrix of energy demand
6: If $TotalRes_{W,i} < 1$ Then $res^{Suit}_{Spp,W,i} = Res\_op_{Spp,Suit,W} \cdot Res\_op_{Spp,Suit,W}$
7: If $TotalRes_{W,i} > 1$ Then Normalize: $res^{Suit}_{Spp,W,i} = res^{Suit}_{Spp,W,i} / TotalRes_{W,i}$
8: If $res^{Suit}_{Spp,W,i} > Res\_op_{Spp,Suit,W}$ Then $res^{Suit}_{Spp,W,i} = Res\_op_{Spp,Suit,W}$
9: Adjust biomass, abundance and size distributions base on $res^{Suit}_{Spp,W,i}$

Table 4. Average latitudinal shift in different simulations. NSI corresponds to simulations where the model does not incorporate species interactions through the size-spectrum, whereas SS denotes the use of the species interactions algorithm. GFDL and ERSEM correspond to two different Earth System Models.

	Latitudinal Shift (km decade^{-1})		
Projection	**All species**	**Demersal**	**Pelagic**
NSI-DBEM GFDL	16.7	14.1	26.0
SS-DBEM GFDL	13.7	12.6	18.4
NSI-DBEM ERSEM	18.1	15.2	28.2
SS-DBEM ERSEM	15.7	15.3	16.9

Figures:

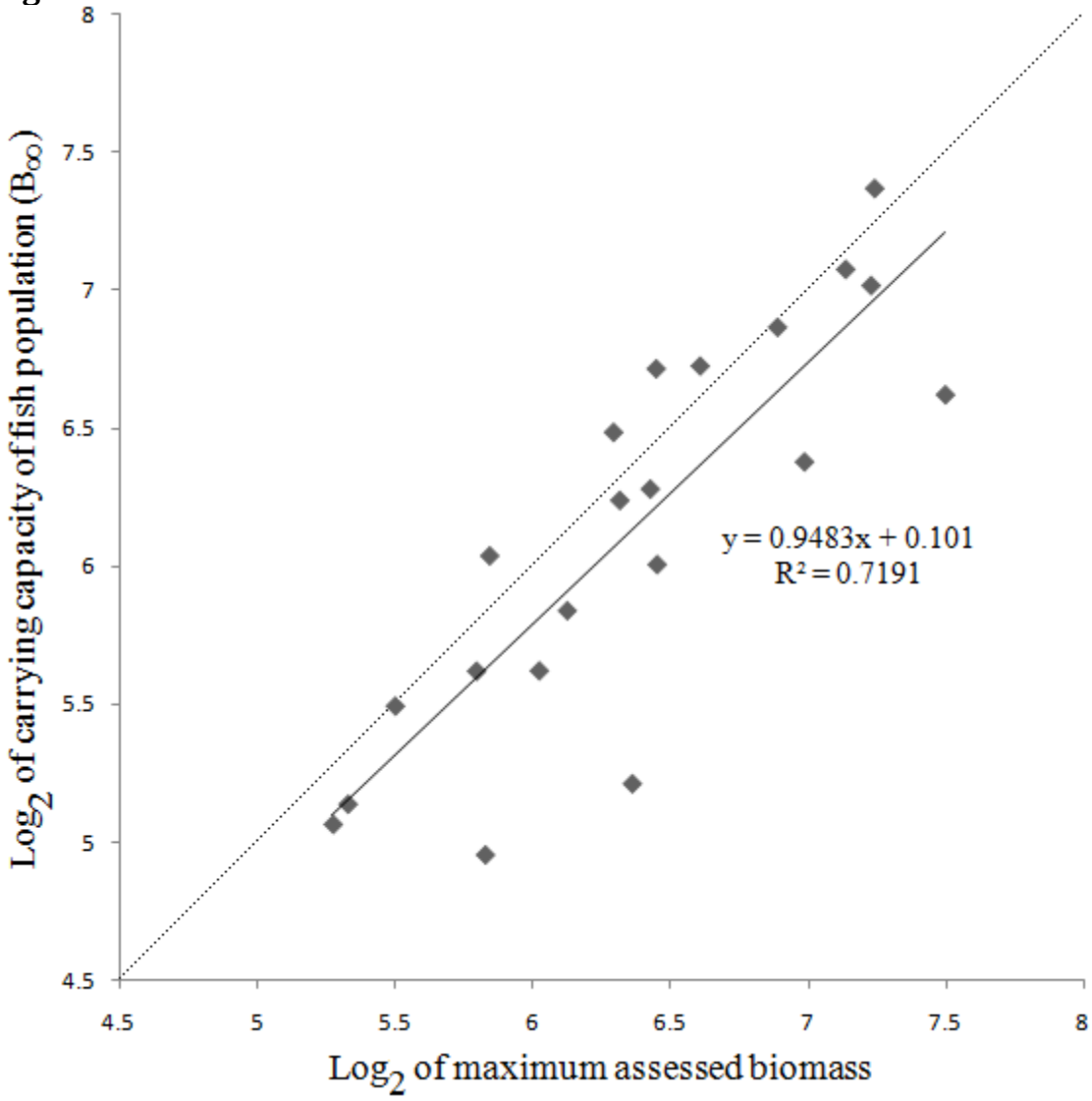

Fig. 1: Relationship between the maximum assessed biomass and the carrying capacity of fish population (B_∞) for 22 species in the 27 FAO area (after removing extreme values, the lowest and highest B_∞).

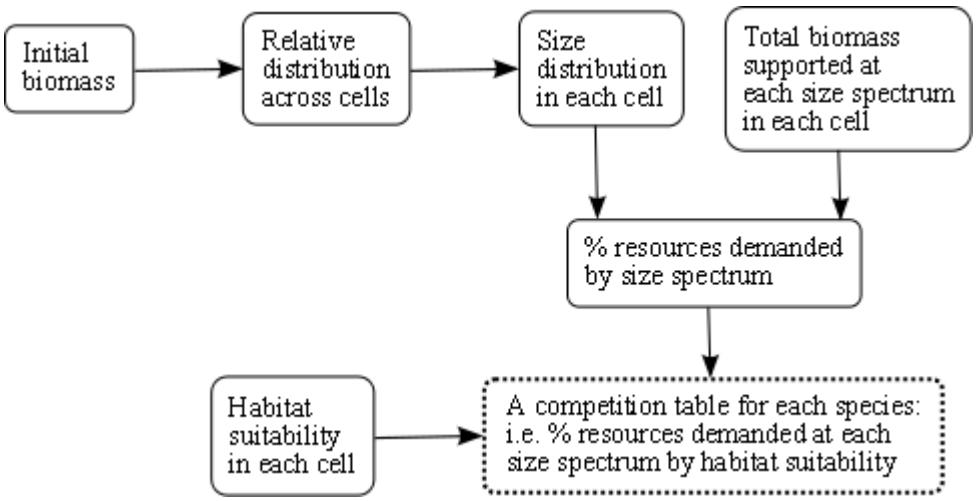

Fig. 2: Diagram of the framework to calculate the matrix of energy demand at each size class for each species.

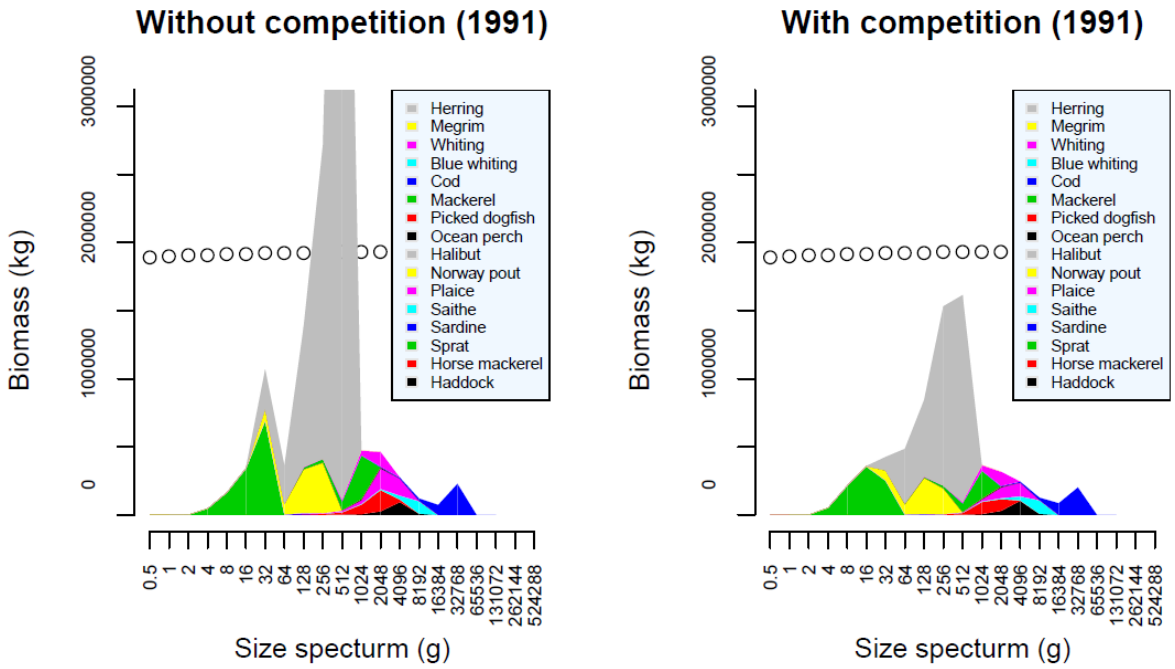

Fig. 3: Species size spectrum distribution in relation to the biomass supported in a single coastal cell (½ degree x ½ degree) used as an example.

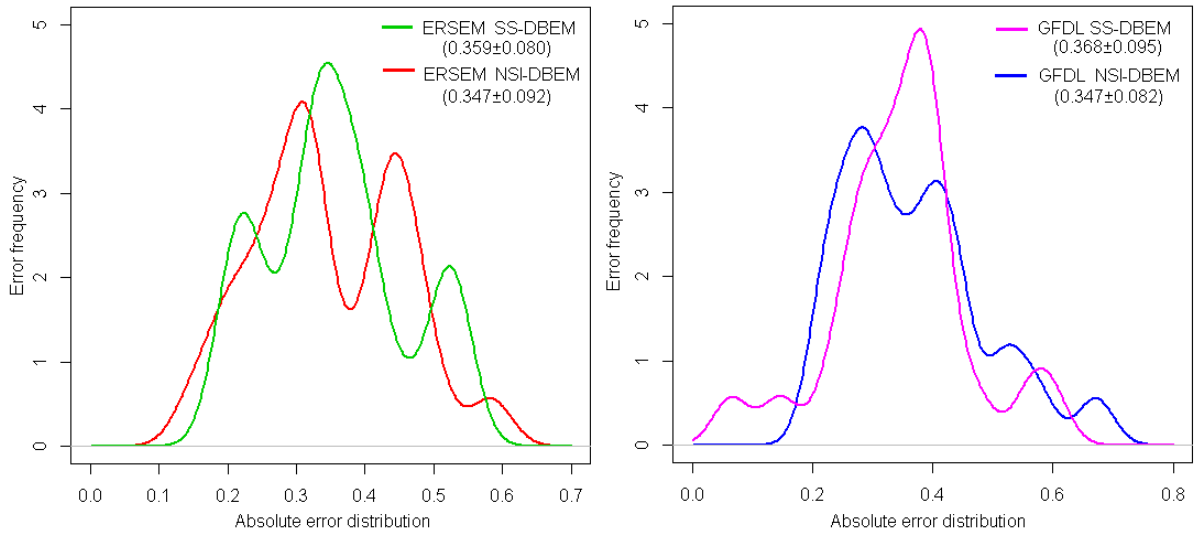

Fig. 4: Distribution of absolute error of predicted biomass for SS-DBEM and NSI-DBEM is reported in relation to the biomass estimated from stock assessments for the 1991 to 2003 period in the Northeast Atlantic (FAO Area 27). The comparison is presented for both Earth System models ERSEM and GFDL in the left and in the right respectively showing in the legend mean and standard deviation of the absolute error. A narrower distribution of error (lower standard deviation) in SS-DBEM is indicative of a higher precision.

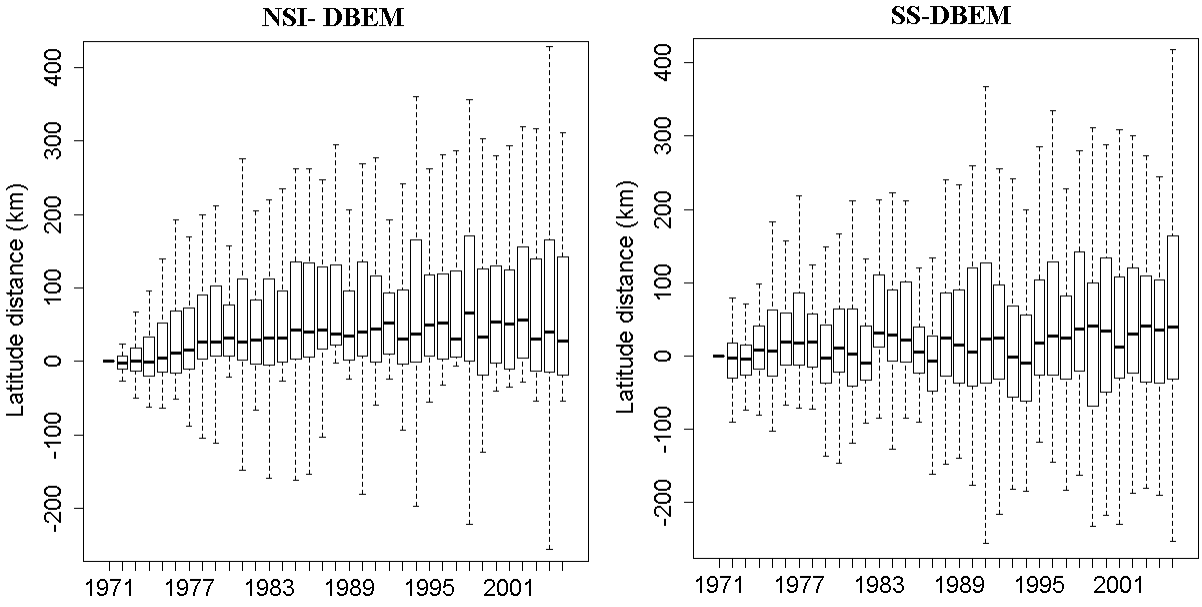

Fig. 5: Predicted latitudinal shift of distribution centroids of 49 species of fishes from 1971 to 2004using ERSEM climatic dataset for the NSI-DBEM and SS-DBEM. The thick dark bar represents the median shift of all the species in a year, the lower and upper boundaries of the box represent the 25% and 75% quartiles, respectively. Positive value indicates polewardshift relative to species distribution in 1971.

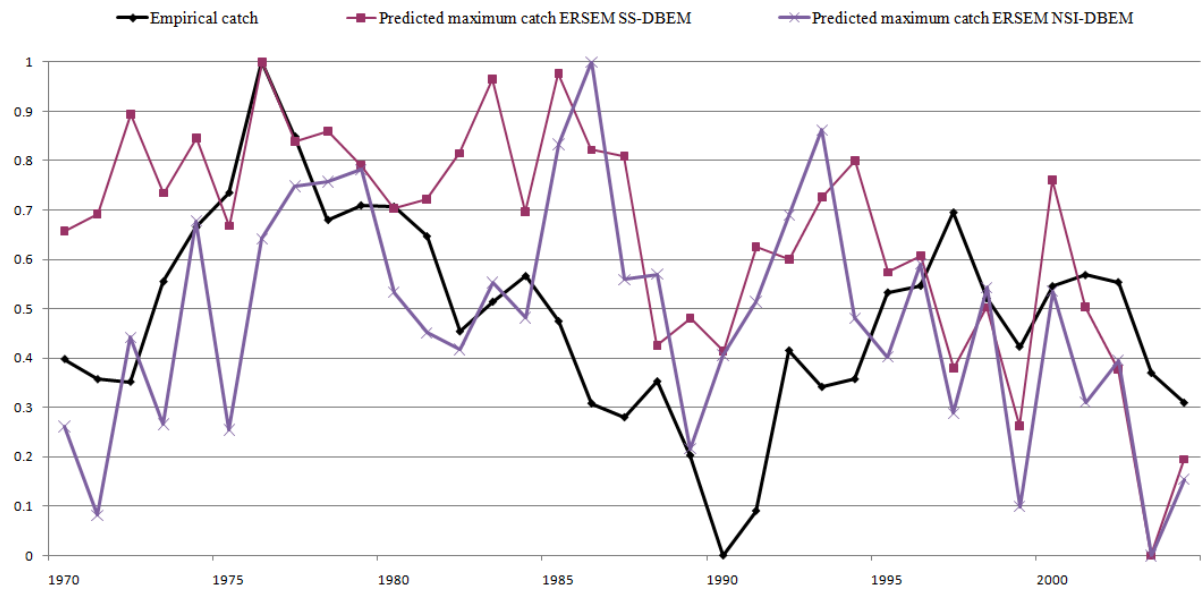

Fig. 6: Predicted changes in maximum catch compared with empirical catch data. Time-series has been normalized between 0 and 1 in order to compare inter-annual variability.